# Autotaxin-lysophosphatidic acid receptor signalling regulates hepatitis C virus replication

Michelle J Farquhar[1*], Isla S Humphreys[1*], Simon A Rudge[2*], Garrick K Wilson[1], Bishnupriya Bhattacharya[1], Maria Ciaccia[2], Ke Hu[1], Qifeng Zhang[2], Laurent Mailly[3], Gary M Reynolds[4], Margaret Aschcroft[5], Peter Balfe[1], Thomas F Baumert[3], Stephanie Roessler[6], Michael JO Wakelam[2**] and Jane A McKeating[1**†]

1. Viral Hepatitis Laboratory, Centre for Human Virology, University of Birmingham, UK.
2. The Babraham Institute, Cambridge, UK.
3. INSERM U1110, University of Strasbourg, 3 Rue Koeberlé, F-67000 Strasbourg, France.
4. NIHR Liver Biomedical Research Unit, University of Birmingham, Birmingham, UK.
5. Cambridge Biomedical Campus, University of Cambridge, Cambridge
6. Institute of Pathology, University Hospital Heidelberg, Heidelberg, Germany.

* Joint first and ** senior authorship.

† Corresponding author Jane A. McKeating, contact information: j.a.mckeating@bham.ac.uk

Tel: (44) 121 414 8173, fax: (44) 121 414 3599

Conflicts of interest: There are no conflict of interest to disclose for any of the authors.

Abbreviations: Alcoholic liver disease (ALD); Autotaxin (ATX); Direct acting antivirals (DAAs); Epstein Barr virus (EBV); hepatitis B virus (HBV); hepatocellular carcinoma (HCC); hepatitis C virus (HCV); HCV pseudoparticle (HCVpp); Hypoxia inducible factor (HIF); lysophosphatidic acid (LPA); lysophosphatidylcholine (LPC); normal liver (NL); primary human hepatocyte (PHH); relative light units (RLU).

Key words: Autotaxin, lipid signalling, hepatitis C virus, hypoxia.

Author involvement: MF, IH, GKW, SR and MC designed and performed the work; KH, BP, QZ and PB performed experiments; SR, LM, MA and TB provided reagents; MJF, SR, JAM and MJOW designed the study and wrote the manuscript.

**Abstract:**

**Background and aims:** Chronic hepatitis C is a global health problem with an estimated 170 million HCV infected individuals at risk of progressive liver disease and hepatocellular carcinoma (HCC). Autotaxin (ATX) is a phospholipase with diverse roles in physiological and pathological processes including inflammation and oncogenesis. Clinical studies have reported increased ATX expression in chronic hepatitis C, however, the pathways regulating ATX and its role in the viral life cycle are not well understood. **Methods**: In vitro hepatocyte and ex vivo liver culture systems along with chimeric humanized liver mice and HCC tissue enabled us to assess the interplay between ATX and the HCV life cycle. **Results**: HCV infection increased hepatocellular ATX RNA and protein expression. HCV infection stabilizes hypoxia inducible factors (HIFs) and we investigated a role for these transcription factors to regulate ATX. *In vitro* studies show that low oxygen increases hepatocellular ATX expression and transcriptome analysis showed a positive correlation between ATX mRNA levels and hypoxia gene score in HCC tumor tissue associated with HCV and other aetiologies. Importantly, inhibiting ATX-lysophosphatidic acid (LPA) signalling reduced HCV replication, demonstrating a positive role for this phospholipase in the viral life cycle. LPA activates phosphoinositide-3-kinase that stabilizes HIF-1α and inhibiting the HIF-signalling pathway abrogates the pro-viral activity of LPA. **Conclusions**: Our data support a model where HCV infection increases ATX expression that supports viral replication and HCC progression.

**Introduction:** Chronic viral hepatitis is a global health problem with at least 170 million hepatitis C virus (HCV) infected individuals at risk of developing liver disease that can progress to hepatocellular carcinoma (HCC). The recent availability of direct acting anti-viral agents can eliminate HCV in up to 90% of patients[1]. However, the high cost of these drugs along with reports of viral genotype resistance, may limit their wide-spread use. Importantly, patients with liver cirrhosis cured of HCV may remain at risk of developing HCC, highlighting the need to understand host pathways playing a role in HCC development[2, 3].

Autotaxin (ATX) is a member of the ectonucleotide pyrophosphatase/phosphodiesterase family of proteins that was identified as a motility-stimulating factor secreted from melanoma cells[4]. ATX hydrolyzes lysophosphatidylcholine (LPC) to lysophosphatidic acid (LPA), a growth factor that activates and signals via a family of six G-protein coupled LPA receptors ($LPA_{1-6}$). The ATX-LPA signalling axis has been reported to play a tumorigenic role in a wide number of cancers and is a candidate for therapeutic intervention[5]. Several studies have reported increased ATX and LPA levels in the plasma of HCV infected subjects that associates with liver fibrosis staging[6-9]. A recent prospective study showed that serum ATX predicts the severity of liver cirrhosis and prognosis of cirrhotic patients[10]. Mazzocca and colleagues reported that HCC secreted LPA increases the trans-differentiation of peritumoral fibroblasts to carcinoma associated fibroblasts that are considered to play a role in tumour proliferation and metastasis[11].

ATX is expressed in many tissues and the mechanisms accounting for increased serum phospholipase activity in chronic hepatitis C and the impact on viral replication are not understood. We show that HCV infection of hepatocyte-derived cells or mice with humanized chimeric livers increases ATX mRNA and protein expression. Infection stabilizes hypoxia inducible factor-1$\alpha$ (HIF-1$\alpha$)[12, 13] and we show that low oxygen increases ATX transcripts in human liver slices, suggesting a pathway for HCV to regulate ATX. We demonstrate a positive association between ATX and hypoxia related gene expression in viral and non-viral HCC, providing an explanation for elevated ATX expression in tumors that are frequently hypoxic. Finally, we demonstrate that ATX-LPA signalling regulates HCV RNA replication via a phosphoinositide 3 kinase (PI3K) dependent pathway, demonstrating a role for lysophospholipids in viral infection. Our data support a model where HCV infection increases hepatocellular ATX expression that promotes viral replication and establishes a paracrine LPA-signalling environment leading to fibrosis and HCC pathogenesis.

**Results**

**HCV infection and low oxygen induce autotaxin expression.** To ascertain whether HCV infection directly regulates ATX expression we selected Huh-7 hepatocyte-derived cells as a permissive target cell that supports HCV replication. *In vitro* tissue culture protocols routinely use media containing bovine serum that contains high levels of ATX that can catalyse LPC-LPA conversion. We therefore performed all experiments under serum-free conditions to limit the confounding effects of *de novo* generated bovine LPA. Huh-7 cells express ATX and the majority of protein is detected in the extracellular media (**Fig.1a**). HCV (strain J6/JFH) infection induced a significant increase in ATX mRNA and protein expression (**Fig.1a**). Experiments to assess the effect of HCV infection on primary human hepatocyte (PHH) ATX expression were inconclusive due to their low permissivity under serum-free conditions required to interrogate human ATX function.

The uPA-SCID human liver chimeric mouse supports HCV infection[14] and enables us to study the effect of viral infection on hepatocellular ATX expression in vivo. Since ATX is likely

to be expressed by multiple cell types in the human liver this murine model provides a unique opportunity to ascertain whether hepatocytes express ATX. All mice engrafted with human hepatocytes express human ATX and infection increased ATX mRNA levels, independent of the hepatocyte donor (**Fig.1b**). In non-transplanted mice we failed to detect ATX expression illustrating both the specificity of the primers for human ATX and demonstrating that HCV-dependent modulation of ATX is of human hepatocyte origin. It is interesting to note that hepatocytes in the transplanted mice express comparable levels of ATX mRNA to Huh-7 cells, however, following isolation and short-term propagation PHHs had lower ATX mRNA levels (**Fig.1c**). We noted a 10-20 fold reduction in mRNA levels of hepatocyte specific markers (Albumin, CYP3A4 and HNF4α) in cultured PHHs during the first 48h of culture, most likely reflecting their de-differentiation. Immunohistochemical staining of the chimeric murine-human livers showed hepatocytes expressing ATX in the HCV infected animals (**Fig.1d**), however, given the secreted nature of this protein we should interpret these data with care with respect to the cellular source of the stained ATX. Next, we sought to analyse ATX RNA levels in HCC from patients diagnosed with HCV, hepatitis B virus (HBV) and alcoholic liver disease (ALD) [15, 16]. Transcriptomic analysis showed a significant increase of ATX in HCV-associated HCC but also in subjects with HBV and ALD compared to normal liver (NL) (**Fig.1e**). A pairwise analysis of tumour and non-tumour tissue from a cohort of 233 Chinese patients with HBV-associated HCC showed that ATX is significantly upregulated in tumour compared to non-tumour tissue (**Fig.1f**).

We observed increased ATX mRNA levels in HCV-infected mice, HCC tumours and Huh-7 cells suggesting that infection perturbs ATX at the transcriptional level. Since HCV can stabilize hypoxia inducible factor 1α (HIF-1-α) [12, 13] we investigated a potential role for this transcription factor to regulate ATX. Under normoxia HIF-α subunits are rapidly targeted for proteosomal degradation by prolyl hydroxylases, however, under low oxygen conditions these hydroxylases are inactivated resulting in stable HIF expression. Huh-7 cells were cultured under normoxic (20%$O_2$) or hypoxic (1%$O_2$) conditions for 24h and ATX mRNA levels along with HIF-target genes VEGF and GLUT1 were quantified. We confirmed HIF-1α expression by Western blotting and observed a significant increase in ATX, VEGF and GLUT1 mRNA and secreted ATX from Huh-7 cells cultured under low oxygen (**Fig.2a**).

To analyse a role for HIF-1α in regulating ATX expression, Huh-7 cells were transfected with a plasmid encoding HIF-1α to express the transcription factor under normoxic conditions. We demonstrated a modest level of HIF-1α expression and increased ATX and VEGF mRNA levels (**Fig.2a**), suggesting a role for HIF in regulating ATX transcription. Further studies investigated the effect of low oxygen on ATX expression in human liver slices. Liver slices from 5 independent donors cultured under normoxic or hypoxic conditions for 24h showed a significant increase in ATX, VEGF and GLUT1 mRNA levels (**Fig.2b**), demonstrating a role for low oxygen in regulating ATX expression in human liver tissue. To ascertain whether low oxygen regulates ATX promoter activity we cloned the published promoter region[7] into a reporter plasmid and quantified luciferase activity in Huh-7 cells cultured under normoxic or hypoxic conditions for 24h. The ATX promoter plasmid showed an approximate 2-log increase in luciferase activity compared to vector alone, however, this was not increased by culturing the cells under hypoxic conditions (**Fig.2c**). As a control Huh-7 expressing a hypoxia responsive element (HRE) reporter, showed a 200-fold increase in luciferase activity (**Fig.2c**). The negligible effect of low oxygen on ATX promoter activity is consistent with the absence of HREs in this region and the lack of HIF-1α binding to this region in HepG2 hepatoma cells by ChIP-SEQ (David Mole, personal communication). Collectively, these data support an indirect role for HIF-1$\alpha$ to regulate ATX transcription.

To understand whether HCV upregulates ATX expression via a HIF-dependent pathway we quantified ATX and VEGF mRNA levels over time and only observed a significant increase in ATX mRNA levels 48h post infection (**Fig.2d**). In contrast, we observed increased VEGF mRNA levels after 24h and they remained elevated for the duration of the experiment (**Fig.2d**). Assuming similar half-lives for these two RNA species these data support a model where HCV stabilized HIF-transcriptional activity precedes ATX upregulation. To validate these conclusions we siRNA silenced HIF-1α in Huh-7 cells to assess its role in viral regulation of ATX and Western blotting confirmed effective silencing under low oxygen conditions (**Fig.2e**). However we failed to infect these cells, suggesting a role for HIF-1α in the HCV life cycle as previously reported[13] but preventing confirmation of this pathway in viral regulation of ATX.

To extend our observations that hypoxia regulates ATX we studied the relationship between ATX and hypoxia gene transcript levels in HCC. van Malenstein *et al* identified a seven gene 'hypoxia signature' that was elevated in HCC[17]. We investigated the expression of these genes in our HCC cohorts. We noted a significant deregulation of five out of seven hypoxia-regulated genes and a significant increase in the hypoxia score in HCC associated with all aetiologies compared to NL (**Supplementary Fig.1**). Since the time of processing liver samples can vary and may result in oxygen deprivation and HIF expression, we selected to study the HBV cohort where tumour and adjacent non-tumour tissue was available, enabling us to limit sampling artefacts and to conduct pairwise comparisons. We observed an increased hypoxia gene score in HCC compared to matched non-tumour tissues (**Fig.3a**). Furthermore, we noted a positive correlation between ATX mRNA and the hypoxia gene signature (**Fig.3b**). Due to the reported association of hypoxia and patient survival, we asked whether ATX gene expression associates with patient outcome[17]. Patients were classified in two groups based on the median difference of ATX expression between tumour and non-tumour tissues. Kaplan-Meier survival curves revealed that patients with high ATX expression had shorter survival times compared to low expression, although this difference was not statistically significant (log-rank p-value) (**Fig.3c**). Thus, we could confirm that the Hypoxia score is increased in HCC tumour tissue compared to adjacent non-tumour tissue and ATX mRNA expression positively correlates with the Hypoxia gene signature supporting a role for hypoxia to regulate ATX-LPA signalling in HCC development.

**Autotaxin-LPA signalling axis in HCV infection.** To investigate a role for ATX in the HCV life cycle we treated Huh-7 cells with HA130, a selective inhibitor of ATX enzymatic activity[18]. HA130 had no effect on Huh-7 viability but significantly reduced LPA levels (**Fig.4a**). LPA is not a single entity and mass spectrometric analysis shows that Huh-7 generate several species of differing acyl chain lengths and degrees of saturation, with 16:0 and 18:1 being the most abundant. Statistical analysis of the results from five independent experiments showed a significant reduction in 18:1, 18:2, 20:4 and 22:6 LPA levels from HA130 treated cells compared to the untreated control. In contrast, HA130 had no significant effect on expression of LPA species 14:0, 16:0 or 18:0 (**Fig.4a**). We observed a dose-dependent HA130 inhibition of HCV J6/JFH and SA13/JFH infection (**Fig.4b**). To confirm these observations, Huh-7 cells were transduced with an shRNA targeting ATX or an irrelevant control. RT-PCR and Western blotting confirmed a reduction in ATX expression and HCV infection (**Fig.4c**). Since off-target effects are a common limitation of gene silencing, we performed a rescue experiment where ATX-silenced cells were transfected to express wild type ($ATX_{wt}$) or a catalytically inactive mutant ($ATX_{T210A}$). Exogenous expression of $ATX_{wt}$ in silenced cells restored infection to levels seen in irrelevant shRNA transduced cells, whereas the $ATX_{T210A}$ mutant had no effect (**Fig.4d**). Of note, expressing $ATX_{wt}$ in shControl or non-transduced Huh-7 cells increased the frequency of HCV infected cells, suggesting that ATX

levels may be limiting. We confirmed that silencing ATX ablated the anti-viral effect of HA130 and exogenous LPA restored HCV infection (**Fig.4e**). To determine whether HCV increased ATX expression drives higher LPA generation we attempted to quantify LPA species in mock and infected samples by mass spectrometry. Unfortunately, the protocol necessary to inactivate the virus prior to analysis, heating the samples at 65$^{o}$C for 10 minutes, caused a 2-3 fold increase in all molecular LPA species most likely explained by heat-induced LPC breakdown. Alternative inactivation protocols involving addition of chloroform/methanol mixtures to the samples were tested but were incompatible with the extraction procedure used for LC-MS analysis.

LPA can regulate cellular proliferation and HA130 treated Huh-7 cells show an increased doubling time from 17h to 23h. To assess whether the anti-viral effect of HA130 is dependent on Huh-7 proliferative status we used DMSO-arrested and differentiated Huh-7 cells[19]. We confirmed that the Huh-7 were cell cycle-arrested and showed increased levels of differentiation markers albumin, CYP3A4 and HNF4-$\alpha$ (**Fig.4f**). The differentiation protocol had no effect on ATX mRNA levels and treating with HA130 reduced HCV infection to a level comparable seen with non-differentiated cells (**Fig.4f**), demonstrating that viral inhibition is not linked to the proliferative status of the target cell.

Since our experiments demonstrate a requirement for the lysophospholipase activity of ATX in HCV infection, we investigated the effect of exogenous LPA (18:1) on Huh-7 permissivity for HCV infection. LPA enhanced HCV infection in a dose-dependent manner (**Fig.5a**). To investigate the receptor dependency of LPA-augmented HCV infection, cells were incubated with LPA in the presence or absence of the $LPA_{1/3}$ antagonist Ki16425[20]. Ki16425 abrogated the pro-viral activity of LPA for HCV infectivity (**Fig.5b**), demonstrating a role for $LPA_1$ or $LPA_3$ in HCV infection. LPA binds and signals through a family of six LPA receptors and Huh-7 cells express mRNA for each of the receptors with the exception of $LPA_4$ at comparable levels to PHHs (**Fig.5c**).

**A role for autotaxin in the HCV lifecycle.** To assess whether ATX has a specific role in HCV entry into hepatocytes, we used lentiviral pseudoparticles expressing HCV E1E2 glycoproteins to measure glycoprotein-receptor entry. We selected HCV strain H77 and 1A38 glycoproteins as they routinely provide the most infectious pseudoparticle stocks[21]. HA130 had no effect on HCVpp infection (**Fig.6a**), similar observations were made with viruses expressing a range of HCV glycoproteins (data not shown). To investigate a role for ATX-LPA signalling in HCV RNA replication we treated Huh-7 cells stably expressing a subgenomic HCV replicon encoding a luciferase reporter (Luc2a-JFH) with HA130 or shATX and noted a significant reduction in luciferase activity (**Fig.6b**). To assess whether HA130 treatment of naïve Huh-7 cells could limit the initiation of HCV RNA replication, Huh-7 cells were transfected with a full-length HCV RNA encoding a secreted gaussia luciferase (JC1GLuc) and we noted a dose-dependent HA130 inhibition of replication (**Fig.6c**). These studies show that inhibiting ATX reduced HCV RNA replication in stably transfected cells and in naïve cells challenged with virus, demonstrating a role for the ATX-LPA signalling in the initiation and maintenance of viral replication.

LPA was reported to stabilize HIF-1α expression in ovarian and colon cancer cells[22] and we investigated a role for HIF-1α in LPA-dependent HCV infection. We show that LPA stabilized HIF-1α under normoxic conditions and increased HRE-transcriptional reporter activity that was inhibited by Ki16425 (**Fig.7a**), demonstrating $LPA_{1/3}$ dependent signalling. We previously reported that the HIF-pathway inhibitor NSC-134754[23] reduced hepatocellular HIF-1α expression and HCV replication[13]. Titration of NSC-134754 identified a sub-saturating

concentration (25nM) that reduced HIF-transcriptional reporter activity with minimal effect on HCV replication and demonstrated a role for the HIF-signalling pathway in the pro-viral activity of LPA (**Fig.7b**). Previous studies reported a role for PI3K activation in LPA-dependent stabilization of HIF-1α[24] and we found that LPA induced AKT phosphorylation in Huh-7 cells (**Fig.7c**). Pre-incubating the cells with the pan PI-3-kinase inhibitor wortmannin (WM) or BYL-719, that selectively targets p110α class IA PI-3-kinase, abrogated HIF-1α expression (**Fig.7d**). In contrast, LPA-stimulated HIF-1α expression was insensitive to the presence of p110β class IA PI3K inhibitor TGX-221 (**Fig.7d**). To establish a role for the PI-3-kinase pathway in LPA-stimulated HCV infection we assessed the ability of these inhibitors to modulate infection. WM and BYL-719 treatments ablated the LPA enhancement of HCV infection whereas TGX-221 had no effect (**Fig.7e**). In summary, these data demonstrate a role for LPA-activated PI-3-kinase signalling in stabilizing HIF-1α that regulates HCV replication (**Fig.7f**).

**Discussion:** Our studies uncover a role for the ATX-LPA signalling axis to positively regulate HCV RNA replication by activating PI3K and stabilizing HIF-1α (**Fig.7f**). Inhibiting ATX activity or LPA signalling reduced HCV replication, providing evidence for an autocrine LPA-feedback loop to promote viral replication. PI3K signalling has been reported to positively regulate HCV replication[25] and suppressing this pathway inhibits HCV replication [26, 27]. We previously reported that low oxygen stabilized HIF promotes HCV infection[13] and our current study showing that silencing HIF-1α limits HCV replication, suggests a role for this pathway in LPA-induced infection. Vassilaki et al reported that low oxygen stimulated HCV replication[28], however, the authors concluded that this phenotype was independent of HIF-1α or HIF-2α that may reflect the use of different Huh-7 cell clones or partial HIF-silencing. Our observation that LPA stabilized hepatocellular HIF-1α and is consistent with reports showing a role for LPA to 'rescue' mesenchymal stromal cells[29] or human CD34+ cells[30] in ischemic disease and are most likely explained by its ability to activate HIF signalling.

We demonstrate a role for low oxygen to regulate ATX mRNA in hepatocyte-derived Huh-7 cells and human liver slices, consistent with reports of increased ATX expression in a variety of tumours that are frequently hypoxic. Importantly, we show a positive association between elevated ATX mRNA levels in HCC and the hypoxia gene score. Transient over-expression of HIF-1α in Huh-7 cells increases ATX mRNA, suggesting an activating role for this transcription factor. However, low oxygen had a minimal effect on ATX promoter activity, in agreement with the lack of HRE sites in this region and suggesting that enhancer regions beyond the published 1.2kb promoter may bind HIFs or that low oxygen regulated factors increase ATX mRNA half-life and/or protein stability. Wu and colleagues reported that TNFα induced a modest 3-fold increase in ATX mRNA levels in HepG2 cells via nuclear factor kappa beta activation[7]. However, we failed to see any evidence for TNFα modulation of ATX promoter activity in Huh-7 cells or human liver slices, suggesting that this may be cell type dependent.

ATX is expressed in many tissues, however the source of elevated ATX in the sera of chronic hepatitis C patients is unknown. Our studies with chimeric liver uPA-SCID mice show that hepatocytes express ATX and HCV infection induces its expression in the absence of any inflammatory response. We confirmed increased ATX transcript levels in HCC tumour tissues from subjects with HCV, HBV and ALD aetiologies, demonstrating that increased ATX expression is not unique to HCV infection. Reports that HBV can stabilize HIF[31] and ALD is associated with hepatic HIF expression[32] lend support to our model that HIFs regulate hepatic ATX expression. In the healthy liver ATX is most likely removed from the circulation by sinusoidal endothelial cells[33], however, during fibrosis phenotypic changes in the

sinusoidal endothelium[34] are likely to impair ATX clearance that may account for the increased expression reported in the fibrotic liver. However, these morphological changes are unlikely to account for the increase in ATX mRNA observed in this study. It is interesting to note that Epstein Barr virus (EBV) infection of Hodgkin lymphoma cells induces ATX expression that augments their proliferation and survival[35]. EBV is an oncogenic virus associated with B-lymphoid and non-lymphoid malignancies that is known to stabilize HIF-1$\alpha$[36], suggesting a common pathway for viruses to activate the ATX-LPA signalling axis.

LPA is not a single entity and exists in several forms with differing acyl chain lengths and degrees of saturation that interact with specific LPA receptors and regulate physiological responses. For example 18:1 LPA activates all receptors, whereas 20:4 LPA shows a higher potency to activate $LPA_3$[37]. Huh-7 cells expressed a range of LPA molecular species and HA130 showed differential effects on the genesis of some LPA species. These results highlight potential differences in the role of LPA molecular species in the viral life cycle, however, this variability may reflect differences in LPC substrate availability and/or lipid phosphate phosphatases that may selectively degrade LPA species.

LPA signals through binding to a family of G-protein coupled receptors that can activate signalling pathways including PI3 kinase and adenylyl cyclase to induce physiological changes including cellular proliferation, anti-apoptosis and migration. Whilst LPA receptor over-expression studies suggest that individual receptors can regulate physiological responses, our understanding of tissue-specific LPA-signalling is limited. PHHs and Huh-7 express all of the LPARs at the mRNA level with the exception of $LPA_4$ in Huh-7 cells. The ability of $LPA_{1/3}$ antagonist Ki16425[20] to limit HCV infection suggests a direct role for $LPA_1$ or $LPA_3$ in viral replication. LPA signalling has been reported to drive chronic wound healing leading to fibrosis and LPA modulators are in development for treating fibrosis[38]. A recent study reported a role for $LPA_6$ in maintaining the proliferative capacity and tumorigenic phenotype of HCC via the transcriptional activation of proto-oncogene *Pim-3*[39], highlight the value of LPA receptor-targeted therapies for treating HCC.

HCC aetiology is multifactorial and the disease is often preceded by other conditions including liver fibrosis and cirrhosis that are associated with HCV, HBV, alcoholic and non-alcoholic hepatitis. The discovery of new therapeutic targets will require a greater understanding of the pathogenic mechanisms underlying the tumorigenic process. Intrahepatic HCC metastases are common and the tumour microenvironment is considered to be pro-metastatic. Reports that elevated serum LPA associate with HCC tumour size and patient survival[11], along with resistance to chemotherapy and radiation-induced cell death[40], provide compelling evidence to consider the ATX-LPA axis as a therapeutic target for treating HCC[41]. The embryonic lethality of ATX null mice[42-44] raised questions on the suitability of ATX as a drug target. However, a recent report from Katsifa and colleagues showing that inducible, ubiquitous genetic deletion of ATX in adult mice, and long-term pharmacologic inhibition were well tolerated limits some of these concerns[45]. In summary, we demonstrate a role for ATX-LPA signalling in the HCV lifecycle, highlighting potential new targets for therapy and the prospect of stratifying therapies for treating viral-associated and non-associated HCC.

**Acknowledgements:** We thank Takaji Wakita for HCV J6/JFH, Jens Bukh for HCV SA13/JFH Charlies Rice for anti-NS5A mAb 9E10, Robert Thimme for Luc2a-JFH replicon cells and Samantha Lissaeur for differentiation protocols. Statistical analysis on mass spectrometric data reported in Fig.4a was performed by Dr. Anne Segonds-Pichon at the bioinformatics facility at the Babraham Institute. Research in the McKeating laboratory was funded by the MRC, NIHR Birmingham Liver BRU, EU FP7 PathCO and H2020 grant Hep-CAR. Research in the Wakelam lab is supported by BBSRC and Hep-CAR. Stephanie Roessler was supported by Hep-CAR, DFG grant RO4673, the Olympia-Morata Programme, a Brigitte-Schieben-Lange Fellowship and a Heidelberg School of Oncology Fellowship.

**Figure legends.**

**Fig.1. HCV induces ATX expression.** (**a**) ATX expression in equal amounts of cellular protein or extracellular media from mock or HCV J6/JFH infected Huh-7 cells at 48h post-infection. Secreted ATX signals were measured by densitometry (annotated on Western blots) and expressed relative to the intracellular pool or mock values. Cells were lysed for total RNA preparation and ATX and GAPDH mRNA levels measured by real time PCR. (**b**) ATX mRNA levels in mock (n=7) or HCV (n=6) infected uPA-SCID mice transplanted with primary human hepatocytes (PHHs), where data is separated according to donor. Serum HCV RNA levels at the time of sacrifice varied from 9,300-34,200 IU/mL. ATX mRNA levels are expressed relative to uninfected cells (**p<0.01). (**c**) ATX mRNA levels in uPA-SCID human liver chimeric mouse tissue (from 3 PHH donors), short-term cultured PHHs (4 donors) and Huh-7 cells expressed relative to GAPDH (**p<0.01). (**d**) Representative immunohistochemical ATX staining in uninfected and HCV infected uPA-SCID liver tissue (x400 magnification). All data sets are representative of at least two independent experiments. (**e**) ATX mRNA levels in HCC tumour tissue from patients with underlying HCV (n=9), HBV (n=8), ALD (n=8), and normal healthy liver tissues (n=7) (*Mann–Whitney U test p<0.05). (**f**) ATX mRNA levels in HBV-associated HCC tumour and paired non-tumour tissue (***Wilcoxon p<0.001).

**Fig.2. Low oxygen regulates ATX expression.** (**a**) Huh-7 cells were cultured under 20% or 1% oxygen for 24h and analysed for HIF-1$\alpha$ expression; ATX, VEGF and Glut1 mRNA levels and secreted ATX (**p<0.01). Huh-7 cells were transfected to express HIF-1$\alpha$ and 48h later assessed for HIF-1$\alpha$ expression, ATX and VEGF mRNA levels (*p<0.05: **p<0.01). ATX protein signals were quantified by densitometry and hypoxic samples expressed relative to normoxic ones. (**b**) Human liver slices from 5 independent donors were incubated under 20% or 1% oxygen for 24h and total RNA screened for ATX, VEGF and GLUT1 mRNA levels (***p<0.001). All gene transcripts are expressed relative to GAPDH housekeeping gene. (**c**) Huh-7 cells expressing ATX promoter-Luc or HRE-Luc were cultured under 20% or 1% oxygen for 24h and luciferase activity measured (**p<0.01: ***p<0.001). All data sets are representative of at least two independent experiments. **(d)** Temporal expression of ATX and VEGF mRNA levels following HCV infection of Huh-7 cells. Infection was assessed by PCR measurement of viral RNA copies at 12, 24 and 48h and were 1.7 x $10^3$, 8.5 x $10^5$ and 4.6 x $10^7$ RNA copies/$10^5$ cells, respectively. (**e**) Huh-7 cells were transfected with siRNA targeting HIF-1$\alpha$ (siHIF) or control (siControl) for 48h, propagated under 1%$O_2$ for 24h to confirm HIF silencing by Western blotting or infected with HCV SA13/JFH for 24h and infection assessed by enumerating the frequency of NS5A expressing cells.

**Fig.3. Association of ATX and hypoxia gene score in HBV-HCC and impact on tumor progression.** (**a**) Hypoxia seven-gene signature in HBV-associates HCC tumour and paired non-tumour tissues (N=233,Wilcoxon p<0.001). (**b**) Correlation of relative ATX difference

between tumour and paired non-tumour tissues and hypoxia seven-gene signature in HBV-associated HCC (Pearson correlation coefficient r =0.2788,p<0.0001). (**c**) Kaplan-Meier survival curves of patients classified by high or low ATX expression between tumour and paired non-tumour tissues (log-rank test,p=0.198).

**Fig.4. Autotaxin promotes HCV infection.** For all experiments Huh-7 cells were cultured under serum-free conditions for 8h prior to experimentation. (**a**) Huh-7 cells were treated with HA130 (100nM) for 24h, LPA expression and cell viability (MTT) measured (*p<0.05). (**b**) Huh-7 were treated with HA130 for 1h prior to infecting with HCV J6/JFH or SA13/JFH for 24h (*p<0.05: ***p<0.001)**.** (**c**) ATX mRNA/protein expression and HCV infection of shATX and Control silenced Huh-7 cells (***p<0.001). (**d**) Control and ATX-silenced Huh-7 cells were transfected with plasmids expressing ATX-wt or ATX-T210A and 48h later ATX secretion assessed by western blot and cells infected with HCV for 24h (*p<0.05: **p<0.01). (**e**) Control or ATX-silenced Huh-7 cells were treated with HA130 (100nM, 1h) or LPA (10uM, 15min) prior to infecting with HCV for 24h (*p<0.05: **p<0.01: ***p<0.001). (**f**) Liver specific differentiation markers (albumin, CYP3A4 and HNF4-$\alpha$) and ATX mRNA levels were measured in untreated and DMSO differentiated growth-arrested Huh-7 cells (***p<0.001). Differentiated cells were incubated with HA130 (100nM) for 1h prior to infecting with HCV SA13/JFH. Infectivity was quantified by measuring the frequency of NS5A expressing cells and expressed relative to untreated cells (***p<0.001). All data sets are representative of at least two independent experiments. Results in (a) show the mean value ± 1 standard error of the mean (SEM), where the P values were obtained using two-way ANOVA accounting for experimental variability on IBM SPSS Statistics Version 22.

**Fig.5. LPA regulates HCV infection.** Huh-7 cells were cultured under serum-free conditions for 8h and (**a**) treated with LPA for 15mins prior to infecting with HCV J6/JFH or SA13/JFH for 24h (*,p<0.05: ***,p<0.001) or (**b**) incubated with Ki16425 (10uM) for 30mins prior to infecting with HCV J6/JFH or SA13/JFH (*p<0.05: **p<0.01: ***p<0.001). Infectivity is expressed relative to the untreated samples and represents the mean of three replicate infections. Infectivity data is representative of two independent experiments. (**c**) LPAR mRNA expression levels in PHH (4 donors) and Huh-7 cells expressed relative to GAPDH.

**Fig.6. ATX-LPA signalling regulates HCV RNA replication.** For all experiments Huh-7 cells were cultured under serum-free conditions for 8h prior to experimentation. (**a**) Huh-7 cells were incubated with HA130 (100nM) for 1h prior to infecting with HCVpp expressing strain H77 or 1A38 envelope glycoproteins for 24h. Infectivity is expressed relative to untreated cells and represents the mean of three replicate infections. (**b**) Huh-7 cells stably expressing the Luc2A-JFH replicon were treated with HA130 (100nM) or transduced to express shControl or shATX for 24h, cells lysed and luciferase activity measured. Data is expressed relative to untreated and represents the mean of three replicate infections (***p<0.001). (**c**) Huh-7 cells were transfected with HCV J6/JFH or a polymerase replication defective genome ($GND^-$) that encodes gaussia luciferase (GLuc) and the cells grown under serum-free conditions for 8h prior to treating with HA130 (100nM). Extracellular media was collected at 0 and 24h post HA130 treatment and luciferase activity measured (***p<0.001). Viral replication is assessed by determining the ratio of J6/JFH/$GND^-$ luciferase activity and represents the mean of three replicate infections.

**Fig.7. LPA stabilizes HIF-1$\alpha$ via a PI3K dependent pathway.** For all experiments Huh-7 cells were cultured under serum-free conditions for 8h prior to experimentation. (**a**) Huh-7 cells expressing HRE-luciferase reporter were treated with LPA (10μM) in the presence or

absence of LPA receptor antagonist Ki16425 (10μM) for 24h. HIF-1α expression was measured by Western blotting (***p <0.001). (**b**) Huh-7 expressing HRE-luciferase reporter were treated with NSC-134754 and cultured under normoxia or 1% oxygen for 24h, lysed and HIF-transcriptional reporter activity measured (relative light units, RLU). Huh-7 cells were treated with 10uM LPA (10μM) in the presence or absence of a sub-saturating dose of NSC-134754 (25nM) for 15mins prior to infecting with HCV SA13/JFH for 24h and infectivity assessed by enumerating NS5A expressing cells. (**c**) Huh-7 cells were treated with LPA (10uM) and cell lysates (40g) probed for phospho-AKT (pAKT) or total AKT (AKT). (**d**) Huh-7 cells were treated with LPA (10μM) in the presence of absence of Ki16425 (10μM), wortmannin (WM) (200nM), BYL-779 (2M) or TGX-221 (50nM) for 24h and cell lysates (40μg) probed for HIF-1α. (**e**) Huh-7 cells were treated with WM (200nM), BYL-779 (2μM) or TGX-221 (50nM) for 15mins prior to infection with HCV J6/JFH in the presence or absence of LPA (10μM). Infectivity is expressed relative to untreated cells and represents the mean of three replicate infections (***p<0.001). HCV infection was measured by enumerating the frequency of NS5A expressing cells 24h post inoculation (***p<0.001). (**f**) Schematic model of ATX-LPA signaling axis in HCV replicative life cycle.

## Materials and Methods

**Cell lines, antibodies and reagents.** Huh-7 (provided by Charles Rice, The Rockefeller University, NY, USA) and 293T (American Type Culture Collection) cells were propagated in Dulbecco's modified Eagle Medium (DMEM) supplemented with 10% FBS and 1% non-essential amino acids (Invitrogen, CA). Huh-7 Luc2a-JFH cells (provided by Robert Thimme, Freiburg)[21] were propagated in the same media supplemented with G418. All cells were grown at 37°C in 5% $CO_2$. For hypoxic conditions cells were cultured at 37°C in a humidified sealed H35 Hypoxystation (Don Wiley Scientific, UK) set to 5% $CO_2$/95% $N_2$/1% $O_2$.

The primary antibodies were: anti-NS5A 9E10 (C. Rice, Rockefeller University, USA); anti-ATX 4FAB; anti-AKT and anti-pAKT (Cell Signaling); anti-HIF-1$\alpha$ (BD Biosciences, Europe). Secondary labelled antibodies: Alexa Fluor 488 goat anti-mouse IgG (Invitrogen, CA); Horseradish peroxidase conjugated sheep anti-mouse and donkey anti-rabbit (GE Healthcare, UK) and anti-rat secondary antibodies (Jackson laboratories). Agonists, inhibitors and antagonists were obtained from the following sources: HA130 (Echelon Biosciences), LPA (Oleoyl-L-alpha-lysophosphatidic acid sodium salt) and wortmannin (Sigma), Ki16425 (Cayman Chemical), BYL-719 (Active Biochem) and TGX-221 (Cayman Chemicals). Cell lysates were quantifed for protein content using a standard Bradford assay and 40$\mu$g of protein analysed. For quantitation of secreted ATX, 50ul of extracellular serum-free conditioned media harvested from a defined cell number was analysed.

Solvents and chemicals for lipids analysis were purchased from the following suppliers: 13:0 LPA (1-tridecanoyl-sn-glycero-3-phosphate in methanol, Avanti Polar lipids-Stratech Scientific Limited), butanol Chromasolv Plus for HPLC and ammonium formate for mass spectrometry (Sigma), acetonitrile and water ultra-gradient grade (Romil), formic acid Optima LC/MS grade (Fisher Scientific).

**uPA-SCID mice infection and immunohistochemical ATX staining.** uPA/SCID-bg mice were transplanted with PHHs at 3 weeks of age by intrasplenic injection as described[14]. Engraftment was assessed by measuring human serum albumin and inoculated with HCV J6/JFH (Jc1) virus. Mice were sacrificed at 16 weeks, the liver recovered and frozen for RNA extraction. Liver samples were fixed in formalin for immunostaining purposes. Experiments were performed at Inserm Unit 1110 animal facility according to local laws and approved by the ethical committee of Strasbourg (number AL/02/19/08/12 and AL/01/18/08/12). Sections (3$\mu$m) of formalin fixed paraffin-embedded liver tissue were deparaffinised, rehydrated and after a low temperature retrieval technique and immunostained for ATX using a Dako Autostainer. Bound antibody was detected with rabbit anti-rat secondary for 15mins, ImmPRESS rabbit secondary for 30mins and visualised using ImmPACT DAB (Vector Labs, UK) and counterstained with Meyers haematoxylin.

**RT-PCR quantification of ATX and HIF-target genes.** Gene amplification was performed in a single tube RT-PCR in accordance with manufacturer's guidelines (CellsDirect kit, Invitrogen, CA) and fluorescence monitored in a 7900HT real time PCR machine (ABI, CA). The housekeeping gene GAPDH was included as an internal control for amplification efficiency and RNA quantification (primer-limited endogenous control, ABI).

**HCC liver samples, clinical data and gene expression data.** We used an Affymetrix U133A2.0 gene expression data set derived from 247 HCC patients as described[16] (GSE14520). Patient samples were obtained with informed consent from patients at the Liver Cancer Institute and Zhongshan Hospital (Fudan University, Shanghai, China). This cohort

contained paired tumour and adjacent non-tumour samples from 232 patients. We also performed gene expression analysis of a German cohort from Heidelberg University Hospital[15]. These tissues included tumour tissue of HCC patients with underlying alcoholic liver disease (ALD, N=8) and HBV (N=8) or HCV (N=9) infection and normal liver samples of patients without HCC or liver cirrhosis (NL, N=7).

**Ex vivo liver slices.** Liver tissue was obtained from patients undergoing resection or transplantation surgery at the Queen Elizabeth Hospital, Birmingham. All liver samples were collected with local National Health Service research ethics committee approval (Walsall LREC 04/Q2708/40) and written informed consent. Cores were cut from the tissue immediately upon receipt in the laboratory. A Krumdieck Tissue Slicer (Alabama Research and Development, USA) was used to section the liver cores. Briefly, the core was placed into the slicer under aseptic conditions and circular slices of ~240μm thickness generated. Slices were immediately transferred into Williams E media (Sigma, UK) supplemented with 1% L-glutamine and 0.5uM insulin.

**Autotaxin promoter activity.** Forward (5'CCGGTACCTGTGCTGCGGAAGAAAAGATG3') and reverse (5'GCCTCGAGGAAAGCCTTTAGCGTG3') primers were used to amplify the ATX promoter region from HepG2 genomic DNA. PCR fragments were cloned into luciferase reporter plasmid pGL4.28 (Promega, Madison, WI) digested with KpnI and XhoI (pGL4.ATX.luc). Huh-7 cells were transfected with pGL4.ATX.luc or pHRE-Luc and 24h later re-seeded in 96 well plates and incubated under 20% $O_2$ or 1% $O_2$ for 24h (Don Whitley Scientific Limited). Cells were lysed and luminescence measured.

**Mass spectrometric LPA analysis.** Huh-7 cells were serum starved for 8h and supernatants harvested, clarified and spiked with 1 ng of 13:0 LPA as an internal standard prior to extraction with 500 ul of butanol. The combined butanol layers were dried under reduced pressure and re-suspended in 100 µl of chloroform/methanol/water 2:5:1 (v/v/v). 5 µl of each sample was analyzed using a Shimadzu Prominence HPLC connected to a QTrap equipped with an electrospray ionisation source (AB Sciex 6500). Separation of LPA species from other interfering lipids such as LPS and LPC was achieved using a Cogent Diamond Hydride column (1 x 150 mm, 4 µm, Microsolv) with the following conditions: 0.2 ml/min flow rate, column temperature 40 oC, autosampler temperature 21 oC. Solvent A was 5 mM ammonium formate aqueous solution pH 3.5 and solvent B was acetonitrile containing 0.1% formic acid and 1% of a 200 mM aqueous solution of ammonium formate pH 3.5. Gradient elution was as follows: isocratic 100% B for 4 minutes, linear decrease 100-75% B in 1.5 minutes, isocratic 75% B for 3.5 minutes, sharp step down to 25% B and isocratic 25% B for 5 minutes (washing step), followed by 10 minutes of re-equilibration with 100% B. The mass spectrometer was operated in negative ion mode using multiple reaction monitoring to record the following transitions: 367.2 → 153.0 for 13:0 LPA, 381.2 → 153.0 for 14:0 LPA, 409.2 → 153.0 for 16:0 LPA, 437.3 → 153.0 for 18:0 LPA, 435.3 → 153.0 for 18:1 LPA, 433.2 → 153.0 for 18:2 LPA, 457.2 → 153.0 for 20:4 LPA, 481.2 → 153.0 for 22:6 LPA. The following optimized MS conditions were used for the analysis: Curtain Gas, 20 psi; Collision Activated Dissociation, Medium; Ion Spray Voltage, -4500 V; Ion Source Temperature, 400 oC; Ion Source Gas 1, 40 psi; Ion Source Gas 2, 30 psi; Declustering Potential, -110 V; Collision Energy, -30 eV; Dwell Time, 50 ms.

**HCV genesis and quantification of infection.** HCV was generated using the Megascript T7 kit (Ambion, Austin, TX), RNA was transcribed in vitro from full-length genomes and electroporated into Huh-7 cells. After 48h cells were serum starved for 8h prior to collecting the serum-free media at 72h post infection and storing at -80°C. Pseudoviruses expressing

luciferase reporters were generated following transfection of 293T cells with a 1:1 ratio of plasmids encoding HIV provirus expressing luciferase and HCV strain 1A38 or H77 E1E2 envelope gps (HCVpp-1A38, HCVpp-H77) or empty vector (Env-pp). At 24h post transfection cells were serum starved and the pseudoparticles harvested 48h post transfection in serum free media.

Target cells were seeded at $1.5x10^4$ cells/$cm^2$ and serum starved for 8h prior to infection with HCV or HCVpp in serum-free media for 24h. HCV infection was assessed following methanol fixation and staining for NS5A with 9E10 antibody; bound antibody was detected with an Alexa 488-conjugated anti-mouse IgG and quantified by enumerating $NS5A^+$ cells. Pseudoparticle infection was quantified by measuring cellular luciferase activity in a luminometer (Berthold Centro LB 960). Relative infectivity was calculated as a percentage of untreated cells and presented ± standard error of the mean (SEM), where the mean infection value of replicate untreated cells wells was defined as 100%.

**Assessing the role of ATX in the HCV life cycle.** Target cells were seeded at 1.5 x $10^4$/$cm^2$ and serum starved for 8h prior to infection. Cells were incubated with HA130 (60min), LPA (in the presence of 0.1mg/ml fatty acid free BSA) (15min), Ki16425 or LPA plus Ki16425 (15min) diluted in serum-free media prior to infecting with HCV or HCVpp for 24h. Huh-7 Luc2a-JFH expressing cells or shATX/shControl transduced cells were seeded at 1.5 x $10^4$/$cm^2$ and serum starved for 8h prior to assay. Cells were untreated or incubated with HA130 for 24h prior to lysis and measuring luciferase. Huh-7 cells were transfected with JC1GLuc for 24h, serum starved for 8h and washed extensively before treating with HA130 for 24h. Extracellular media was harvested, heat inactivated and luciferase activity measured.

**Autotaxin silencing, rescue, and HIF-1α silencing.** 293T cells were transfected with plasmids plKO.1 shATX (TRCN0000048993) or plKO.1 control (Open Biosystems) plus p8.2 gag pol and VSV-G and 72h later lentiviral particles harvested and used to transduce Huh-7. Cells were cultured in the presence of puromycin and ATX knockdown determined by Western blotting. shControl and shATX stable expressing Huh-7 cells were transfected with His-tagged wild type ATX (ATX-wt) or T210A ATX mutant (ATX-T210A) (Addgene plasmid 17839 and 17840 respectively) for 24h prior to seeding cells for infection studies. Huh-7 cells were transfected using Dharmafect according to manufactures instructions with siHIF-1α (siHIF) or shControl (Thermoscientific, UK) and incubated for 48h prior assessing HIF-1α by Western blot or infecting with HCV.

**Statistical analysis.** Results are shown as the mean value ± 1 standard deviation (SD) except where stated otherwise, all data were tested for fit a Gaussian assumptions and analyses performed using either Student's t-test (pairwise comparisons) or Kruskal-Wallis One-Way ANOVA with Dunn's test (for multiple comparisons), except where stated otherwise, in Graph Pad Prism 6 (GraphPad, USA), with a P value of $<0.05$ considered statistically significant. Expression differences between HCC and non-tumorous liver samples were assessed by Wilcoxon signed-rank test for paired samples. Kaplan-Maier curves and log-rank test were performed with Graph Pad Prism 6. Differential expression in aetiology groups of the German cohort were analysed by nonparametric Mann-Whitney U tests. The hypoxia score was calculated as previously reported[17].

**References:**


[1] Pawlotsky JM. New hepatitis C virus (HCV) drugs and the hope for a cure: concepts in anti-HCV drug development. Seminars in liver disease 2014;34:22-29.

[2] van der Meer AJ, Veldt BJ, Feld JJ, Wedemeyer H, Dufour JF, Lammert F, et al. Association between sustained virological response and all-cause mortality among patients with chronic hepatitis C and advanced hepatic fibrosis. JAMA 2012;308:2584-2593.

[3] **Reig M**, **Marino Z**, Perello C, Inarrairaegui M, Ribeiro A, Lens S, et al. Unexpected early tumor recurrence in patients with hepatitis C virus -related hepatocellular carcinoma undergoing interferon-free therapy: a note of caution. Journal of hepatology 2016.

[4] Stracke ML, Krutzsch HC, Unsworth EJ, Arestad A, Cioce V, Schiffmann E, et al. Identification, purification, and partial sequence analysis of autotaxin, a novel motility-stimulating protein. The Journal of biological chemistry 1992;267:2524-2529.

[5] **Barbayianni E**, **Kaffe E**, Aidinis V, Kokotos G. Autotaxin, a secreted lysophospholipase D, as a promising therapeutic target in chronic inflammation and cancer. Prog Lipid Res 2015;58:76-96.

[6] Schlatzer DM, Sugalski JM, Chen Y, Barnholtz-Sloan J, Davitkov P, Hazlett FE, et al. Plasma proteome analysis reveals overlapping, yet distinct mechanisms of immune activation in chronic HCV and HIV infections. Journal of acquired immune deficiency syndromes 2013;63:563-571.

[7] Wu JM, Xu Y, Skill NJ, Sheng H, Zhao Z, Yu M, et al. Autotaxin expression and its connection with the TNF-alpha-NF-kappaB axis in human hepatocellular carcinoma. Molecular cancer 2010;9:71.

[8] Cooper AB, Wu J, Lu D, Maluccio MA. Is autotaxin (ENPP2) the link between hepatitis C and hepatocellular cancer? Journal of gastrointestinal surgery : official journal of the Society for Surgery of the Alimentary Tract 2007;11:1628-1634; discussion 1634-1625.

[9] Kondo M, Ishizawa T, Enooku K, Tokuhara Y, Ohkawa R, Uranbileg B, et al. Increased serum autotaxin levels in hepatocellular carcinoma patients were caused by background liver fibrosis but not by carcinoma. Clinica chimica acta; international journal of clinical chemistry 2014;433:128-134.

[10] Pleli T, Martin D, Kronenberger B, Brunner F, Koberle V, Grammatikos G, et al. Serum autotaxin is a parameter for the severity of liver cirrhosis and overall survival in patients with liver cirrhosis--a prospective cohort study. PloS one 2014;9:e103532.

[11] Mazzocca A, Dituri F, Lupo L, Quaranta M, Antonaci S, Giannelli G. Tumor-secreted lysophostatidic acid accelerates hepatocellular carcinoma progression by promoting differentiation of peritumoral fibroblasts in myofibroblasts. Hepatology 2011;54:920-930.

[12] Nasimuzzaman M, Waris G, Mikolon D, Stupack DG, Siddiqui A. Hepatitis C virus stabilizes hypoxia-inducible factor 1alpha and stimulates the synthesis of vascular endothelial growth factor. Journal of virology 2007;81:10249-10257.

[13] Wilson GK, Brimacombe CL, Rowe IA, Reynolds GM, Fletcher NF, Stamataki Z, et al. A dual role for hypoxia inducible factor-1alpha in the hepatitis C virus lifecycle and hepatoma migration. Journal of hepatology 2012;56:803-809.

[14] Mercer DF, Schiller DE, Elliott JF, Douglas DN, Hao C, Rinfret A, et al. Hepatitis C virus replication in mice with chimeric human livers. Nature medicine 2001;7:927-933.

[15] Neumann O, Kesselmeier M, Geffers R, Pellegrino R, Radlwimmer B, Hoffmann K, et al. Methylome analysis and integrative profiling of human HCCs identify novel protumorigenic factors. Hepatology 2012;56:1817-1827.

[16] Roessler S, Jia HL, Budhu A, Forgues M, Ye QH, Lee JS, et al. A unique metastasis gene signature enables prediction of tumor relapse in early-stage hepatocellular carcinoma patients. Cancer research 2010;70:10202-10212.

[17] van Malenstein H, Gevaert O, Libbrecht L, Daemen A, Allemeersch J, Nevens F, et al. A seven-gene set associated with chronic hypoxia of prognostic importance in hepatocellular carcinoma. Clinical cancer research : an official journal of the American Association for Cancer Research 2010;16:4278-4288.
[18] Albers HM, Dong A, van Meeteren LA, Egan DA, Sunkara M, van Tilburg EW, et al. Boronic acid-based inhibitor of autotaxin reveals rapid turnover of LPA in the circulation. Proc Natl Acad Sci U S A 2010;107:7257-7262.
[19] Sainz B, Jr., Chisari FV. Production of infectious hepatitis C virus by well-differentiated, growth-arrested human hepatoma-derived cells. Journal of virology 2006;80:10253-10257.
[20] Ohta H, Sato K, Murata N, Damirin A, Malchinkhuu E, Kon J, et al. Ki16425, a subtype-selective antagonist for EDG-family lysophosphatidic acid receptors. Molecular pharmacology 2003;64:994-1005.
[21] Bailey JR, Wasilewski LN, Snider AE, El-Diwany R, Osburn WO, Keck Z, et al. Naturally selected hepatitis C virus polymorphisms confer broad neutralizing antibody resistance. J Clin Invest 2015;125:437-447.
[22] Lee SJ, No YR, Dang DT, Dang LH, Yang VW, Shim H, et al. Regulation of hypoxia-inducible factor 1alpha (HIF-1alpha) by lysophosphatidic acid is dependent on interplay between p53 and Kruppel-like factor 5. The Journal of biological chemistry 2013;288:25244-25253.
[23] Baker LC, Boult JK, Walker-Samuel S, Chung YL, Jamin Y, Ashcroft M, et al. The HIF-pathway inhibitor NSC-134754 induces metabolic changes and anti-tumour activity while maintaining vascular function. Br J Cancer 2012;106:1638-1647.
[24] Lee J, Park SY, Lee EK, Park CG, Chung HC, Rha SY, et al. Activation of hypoxia-inducible factor-1alpha is necessary for lysophosphatidic acid-induced vascular endothelial growth factor expression. Clinical cancer research : an official journal of the American Association for Cancer Research 2006;12:6351-6358.
[25] Mannova P, Beretta L. Activation of the N-Ras-PI3K-Akt-mTOR pathway by hepatitis C virus: control of cell survival and viral replication. Journal of virology 2005;79:8742-8749.
[26] Chen MH, Lee MY, Chuang JJ, Li YZ, Ning ST, Chen JC, et al. Curcumin inhibits HCV replication by induction of heme oxygenase-1 and suppression of AKT. International journal of molecular medicine 2012;30:1021-1028.
[27] Pisonero-Vaquero S, Garcia-Mediavilla MV, Jorquera F, Majano PL, Benet M, Jover R, et al. Modulation of PI3K-LXRalpha-dependent lipogenesis mediated by oxidative/nitrosative stress contributes to inhibition of HCV replication by quercetin. Laboratory investigation; a journal of technical methods and pathology 2014;94:262-274.
[28] Vassilaki N, Kalliampakou KI, Kotta-Loizou I, Befani C, Liakos P, Simos G, et al. Low oxygen tension enhances hepatitis C virus replication. Journal of virology 2013;87:2935-2948.
[29] Binder BY, Genetos DC, Leach JK. Lysophosphatidic acid protects human mesenchymal stromal cells from differentiation-dependent vulnerability to apoptosis. Tissue engineering Part A 2014;20:1156-1164.
[30] Kostic I, Fidalgo-Carvalho I, Aday S, Vazao H, Carvalheiro T, Graos M, et al. Lysophosphatidic acid enhances survival of human CD34(+) cells in ischemic conditions. Scientific reports 2015;5:16406.
[31] Liu LP, Hu BG, Ye C, Ho RL, Chen GG, Lai PB. HBx mutants differentially affect the activation of hypoxia-inducible factor-1alpha in hepatocellular carcinoma. Br J Cancer 2014;110:1066-1073.
[32] Szabo G. Gut-liver axis in alcoholic liver disease. Gastroenterology 2015;148:30-36.
[33] Jansen S, Andries M, Vekemans K, Vanbilloen H, Verbruggen A, Bollen M. Rapid clearance of the circulating metastatic factor autotaxin by the scavenger receptors of liver sinusoidal endothelial cells. Cancer letters 2009;284:216-221.
[34] Muro H, Shirasawa H, Kosugi I, Nakamura S. Defect of Fc receptors and phenotypical changes in sinusoidal endothelial cells in human liver cirrhosis. The American journal of pathology 1993;143:105-120.

[35] Baumforth KRN, Flavell JR, Reynolds GM, Davies G, Pettit TR, Wei WB, et al. Induction of autotaxin by the Epstein-Barr virus promotes the growth and survival of Hodgkin lymphoma cells. Blood 2005;106:2138-2146.
[36] Kondo S, Seo SY, Yoshizaki T, Wakisaka N, Furukawa M, Joab I, et al. EBV latent membrane protein 1 up-regulates hypoxia-inducible factor 1alpha through Siah1-mediated down-regulation of prolyl hydroxylases 1 and 3 in nasopharyngeal epithelial cells. Cancer research 2006;66:9870-9877.
[37] Tigyi G. Aiming drug discovery at lysophosphatidic acid targets. Br J Pharmacol 2010;161:241-270.
[38] Budd DC, Qian Y. Development of lysophosphatidic acid pathway modulators as therapies for fibrosis. Future medicinal chemistry 2013;5:1935-1952.
[39] Mazzocca A, Dituri F, De Santis F, Filannino A, Lopane C, Betz RC, et al. Lysophosphatidic acid receptor LPAR6 supports the tumorigenicity of hepatocellular carcinoma. Cancer research 2015;75:532-543.
[40] Brindley DN, Lin FT, Tigyi GJ. Role of the autotaxin-lysophosphatidate axis in cancer resistance to chemotherapy and radiotherapy. Biochimica et biophysica acta 2013;1831:74-85.
[41] Barbayianni E, Magrioti V, Moutevelis-Minakakis P, Kokotos G. Autotaxin inhibitors: a patent review. Expert opinion on therapeutic patents 2013;23:1123-1132.
[42] van Meeteren LA, Ruurs P, Stortelers C, Bouwman P, van Rooijen MA, Pradere JP, et al. Autotaxin, a secreted lysophospholipase D, is essential for blood vessel formation during development. Molecular and cellular biology 2006;26:5015-5022.
[43] Tanaka M, Okudaira S, Kishi Y, Ohkawa R, Iseki S, Ota M, et al. Autotaxin stabilizes blood vessels and is required for embryonic vasculature by producing lysophosphatidic acid. The Journal of biological chemistry 2006;281:25822-25830.
[44] Fotopoulou S, Oikonomou N, Grigorieva E, Nikitopoulou I, Paparountas T, Thanassopoulou A, et al. ATX expression and LPA signalling are vital for the development of the nervous system. Developmental biology 2010;339:451-464.
[45] Katsifa A, Kaffe E, Nikolaidou-Katsaridou N, Economides AN, Newbigging S, McKerlie C, et al. The Bulk of Autotaxin Activity Is Dispensable for Adult Mouse Life. PloS one 2015;10:e0143083.

Figure 1

Click here to download high resolution image

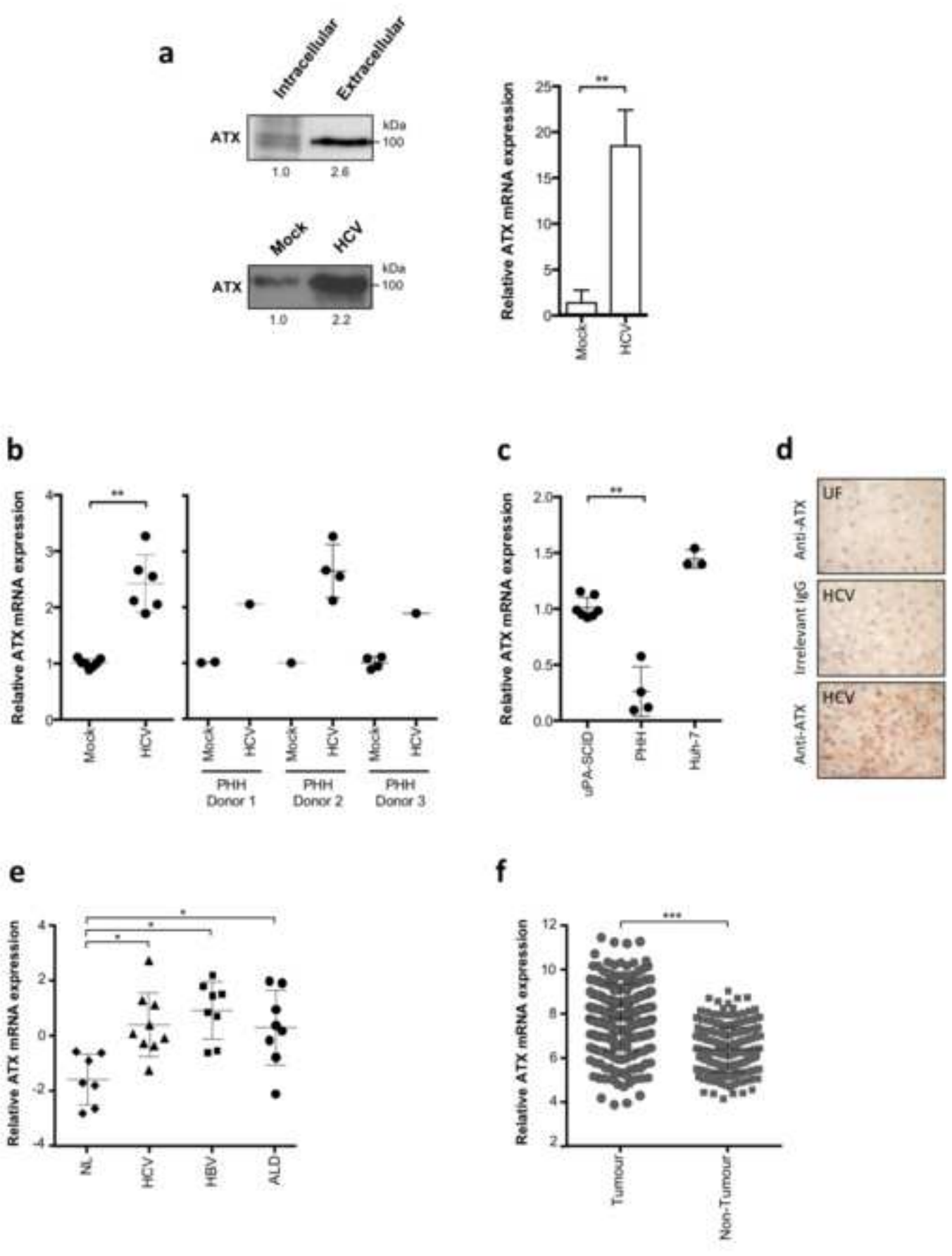

**Figure 2**

Click here to download high resolution image

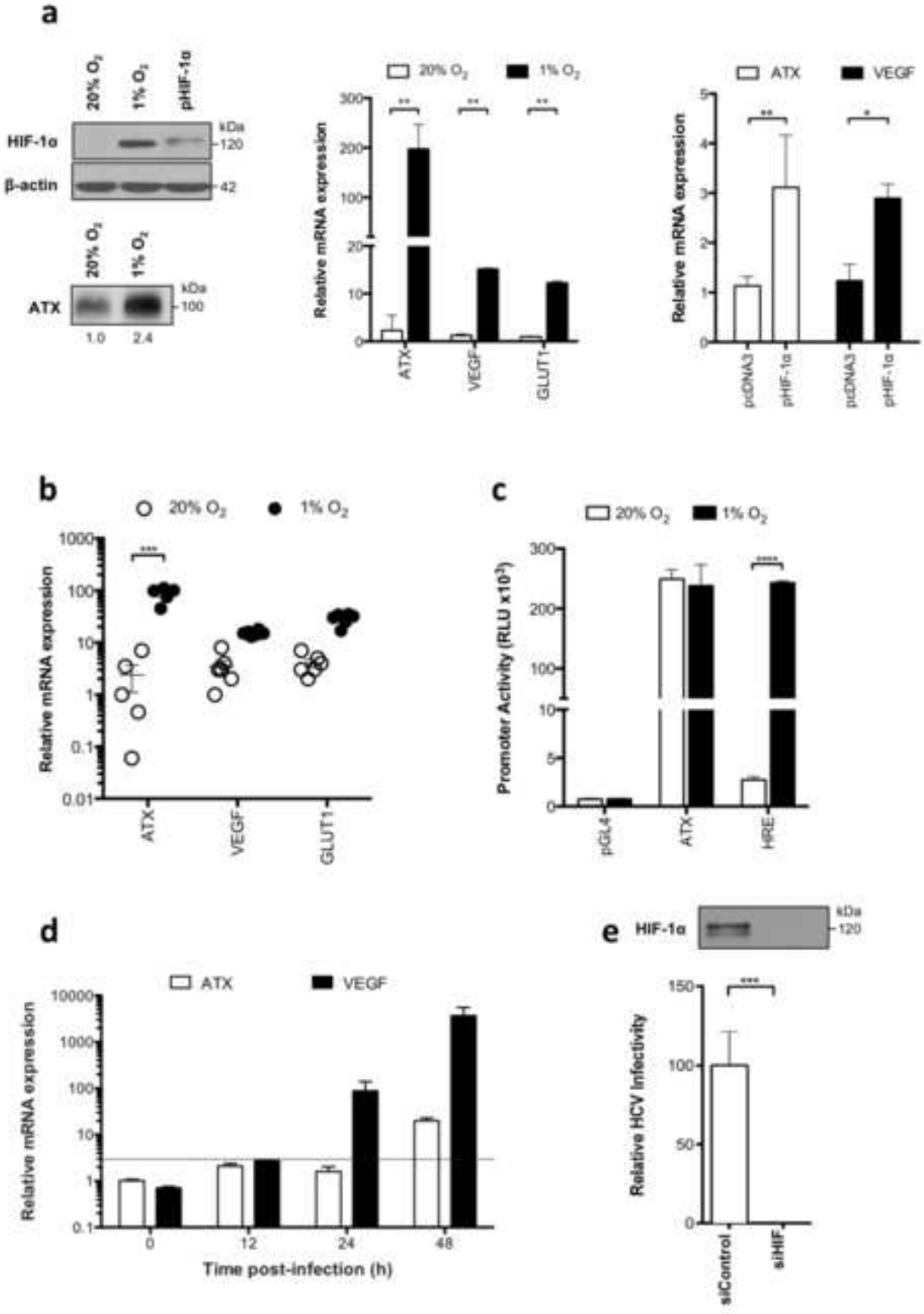

**Figure 3**

Click here to download high resolution image

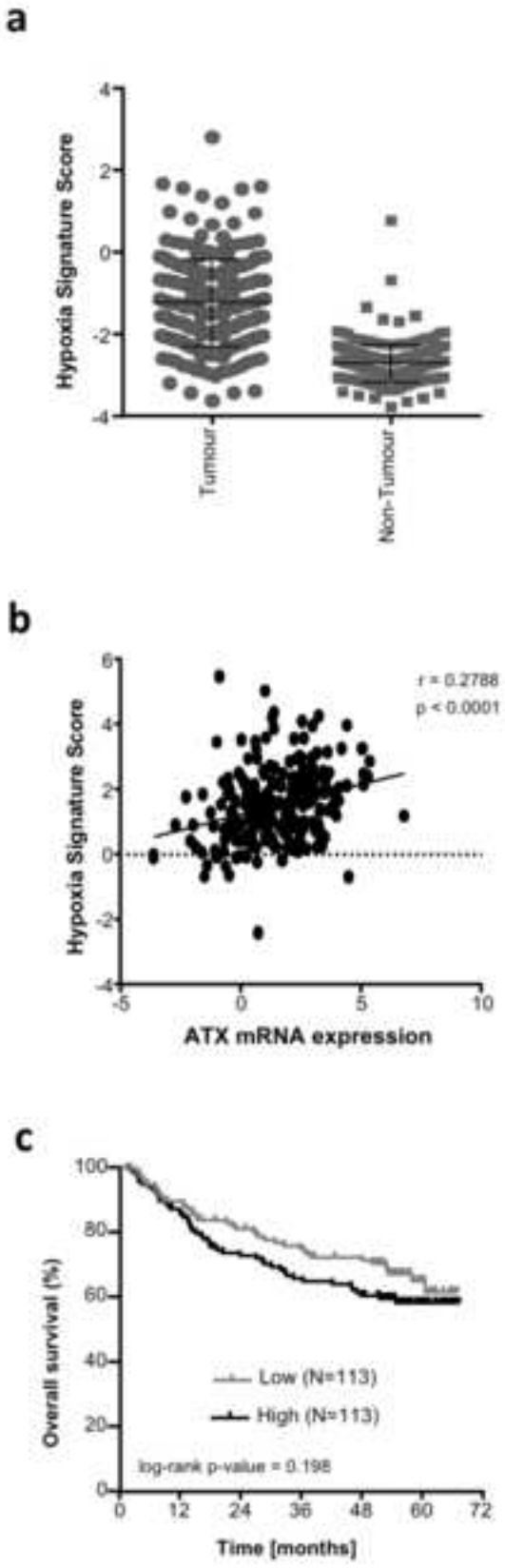

Figure 4

Click here to download high resolution image

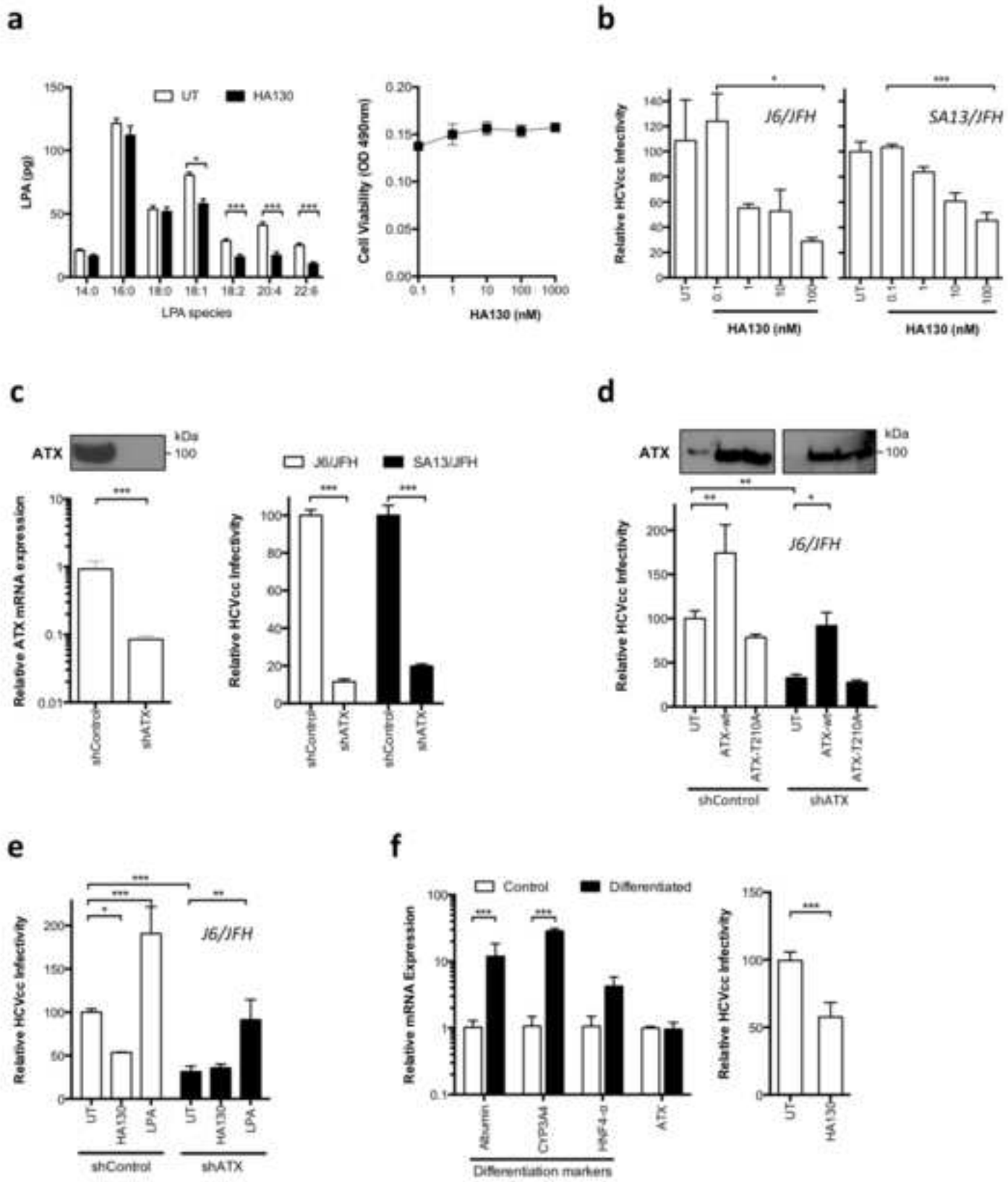

**Figure 5**

**Click here to download high resolution image**

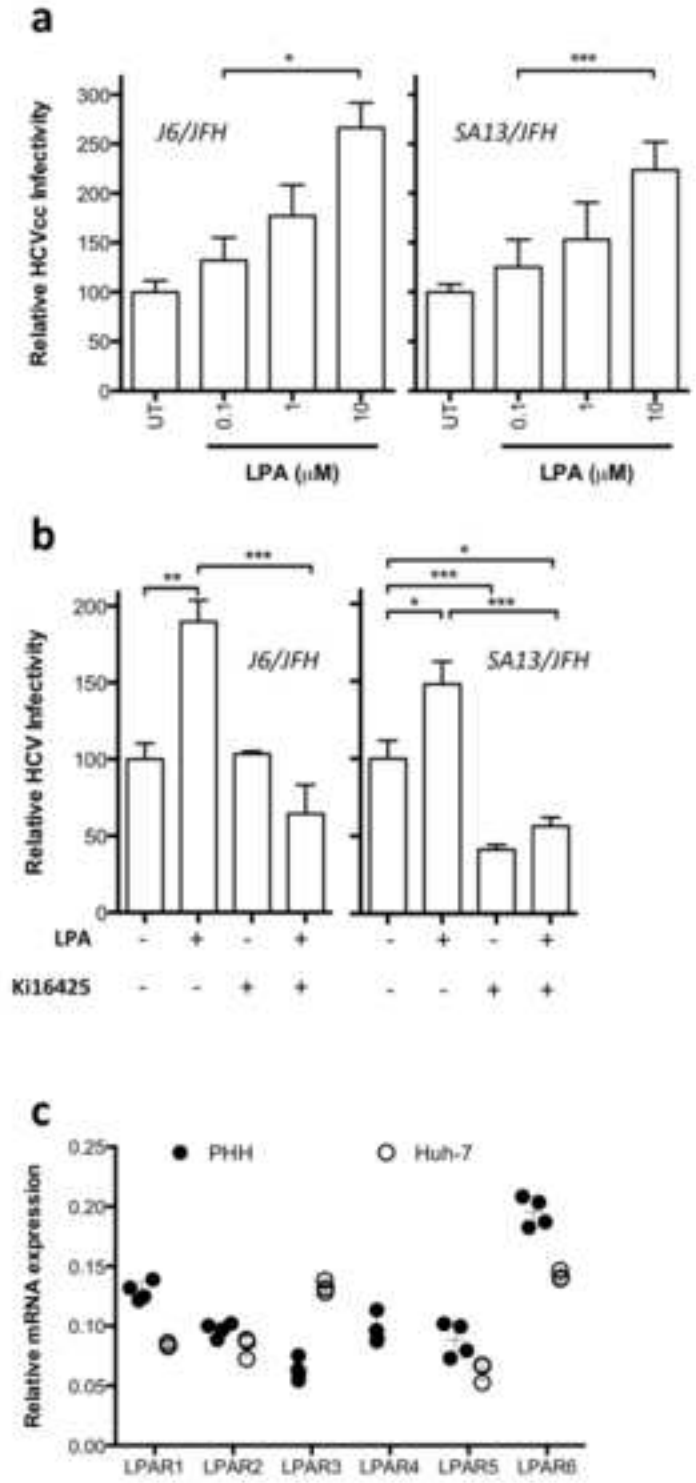

**Figure 6**

**Click here to download high resolution image**

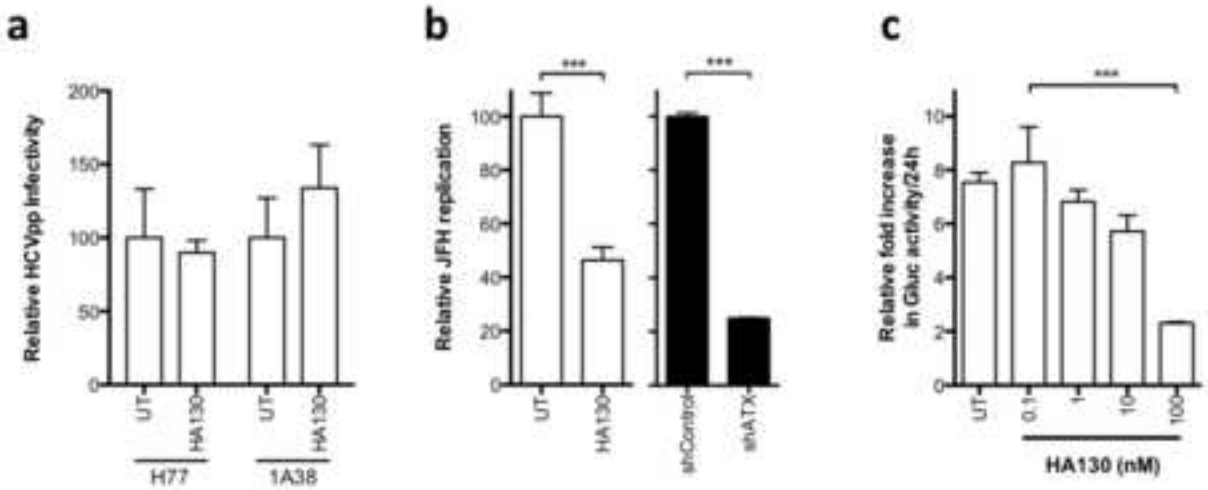

Figure 7

Click here to download high resolution image

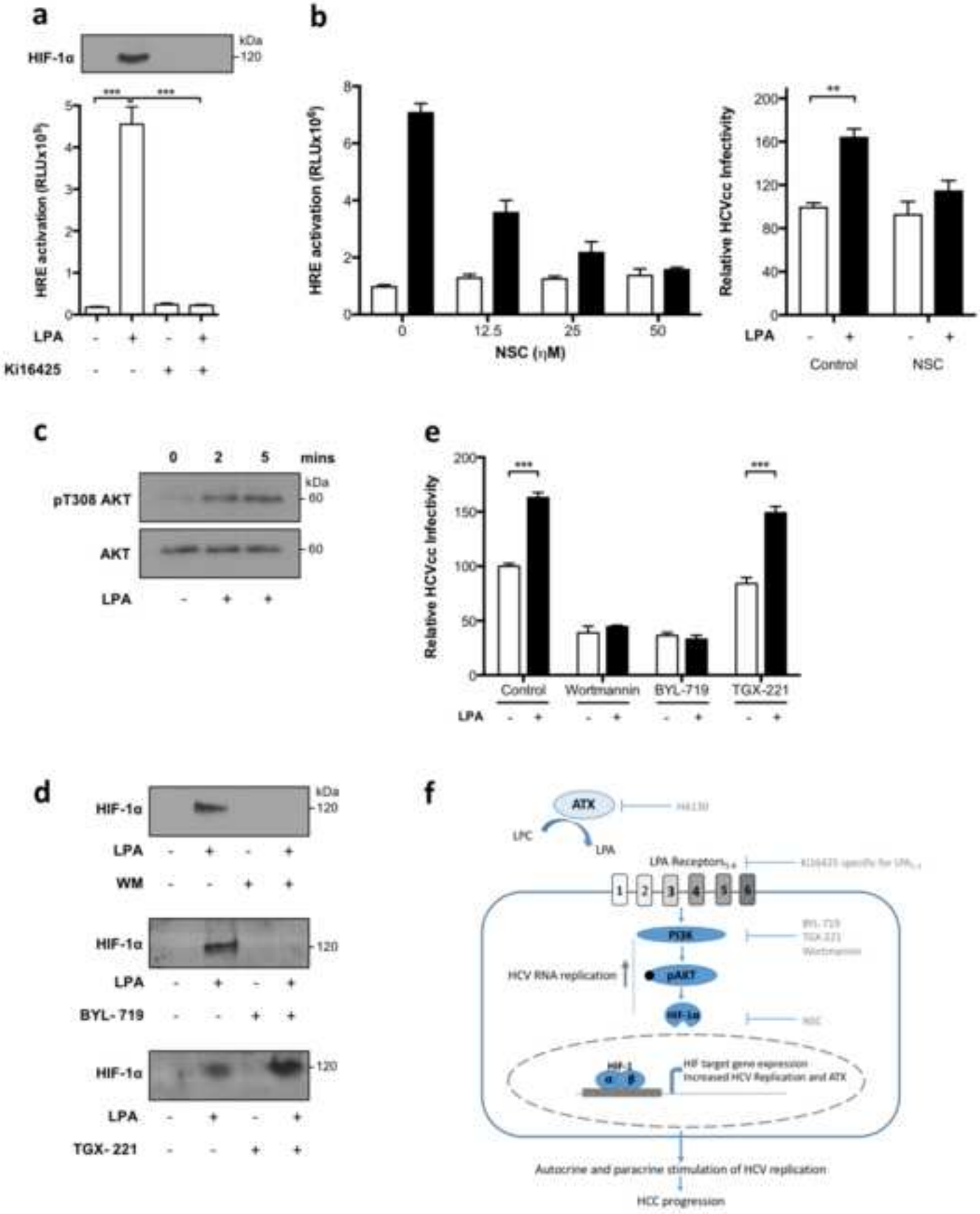

*Graphical Abstract

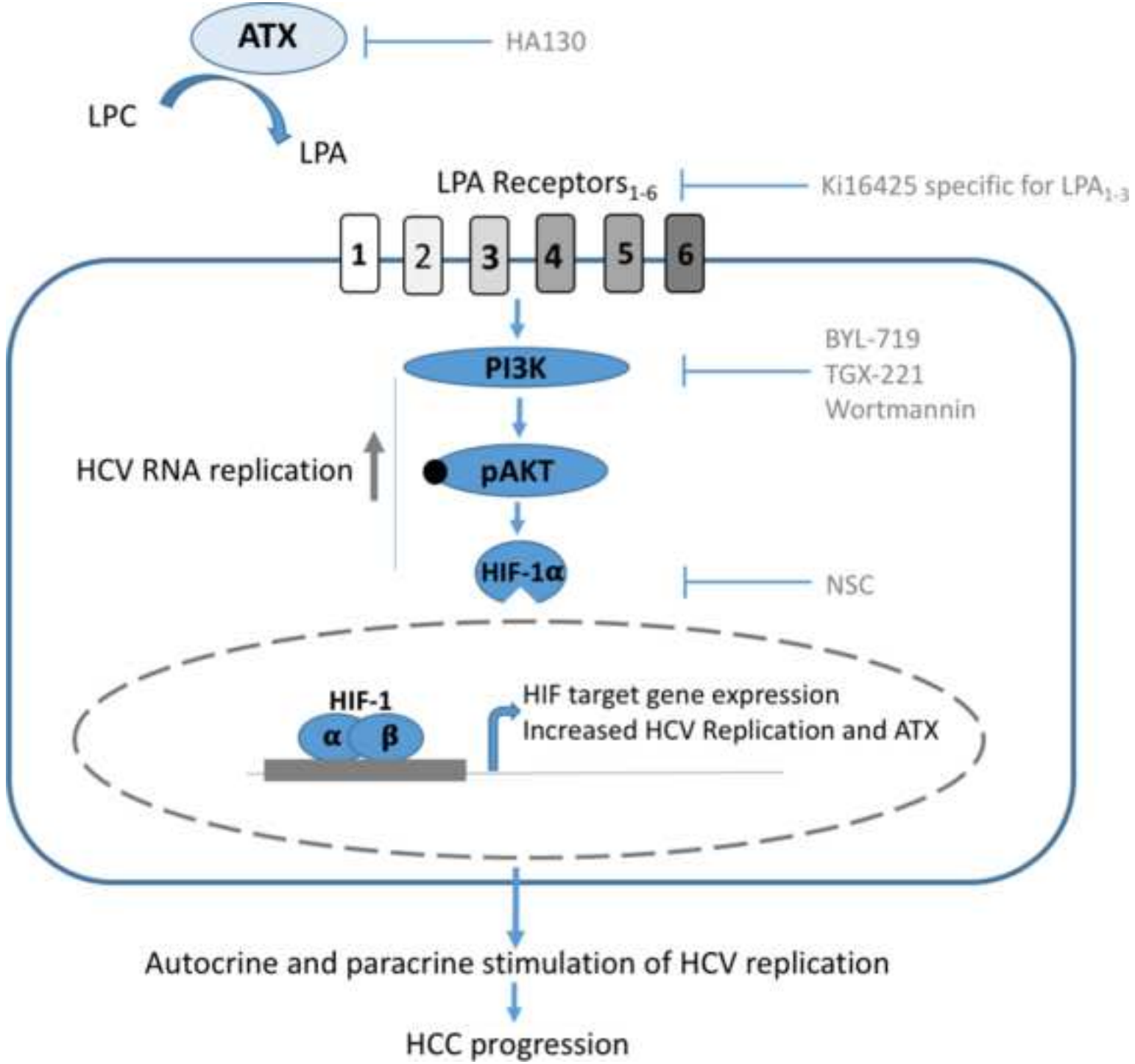

**Supplementary material**

**Click here to download Supplementary material: Supplementary Figure.docx**